Modeling a Mains connected PWM Converter with Voltage-Oriented Control

Anton Haumer Christian Kral
AIT Austrian Institute of Technology GmbH
Giefinggasse 2, 1210 Vienna, Austria

Abstract

The majority of industrial controlled induction machine drives are connected to the mains via a diode bridge. However, if reduction of harmonic currents and / or regenerative operation is desired, replacing the diode bridge by an active front-end (AFE) is required. This paper describes two models of an AFE: a power balance model disregarding switching effects, and an ideal switching model of a pulse width modulation (PWM) converter. Both models are controlled utilizing space phasors in a voltage oriented reference frame. Voltage oriented control (VOC) of the mains converter can be compared with field oriented control (FOC) of a machine converter. Design and parametrization of the main parts—synchronization with mains voltage, current controller and DC voltage controller—are described in detail. Additionally, simulation results proving the implementation and demonstrating possible investigations as well as an outlook on further enhancements are presented.

Keywords: Active Front-End, PWM Converter, Voltage-Oriented Control

1 Introduction

The standard solution for industrial controlled drives consists of an induction machine, fed by a voltage source inverter. The drive usually is field-oriented controlled, as described e.g. in [1]. In many cases, the DC link is connected to the mains via a diode bridge due to cost saving reasons. However, some goals cannot be fulfilled by a diode bridge:

- Regenerative / recuperative operation
- Reduction of harmonic currents
- Control of reactive power

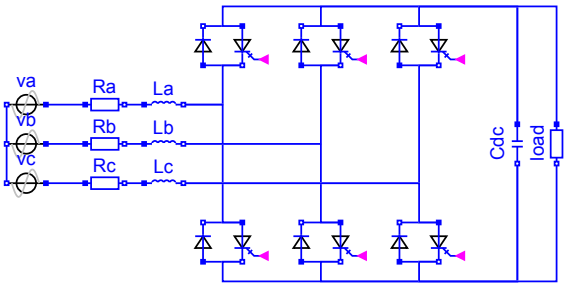

Figure 1: Model of an AFE with PWM converter

Replacing the diode bridge by an IGBT bridge as shown in Fig. 1 allows to address these topics. Between the mains and the AFE a mains reactor has to be used to limit the current slope and current harmonics, respectively.
The control of such an active front-end can be designed in several ways, as described in [2, 3, 4, 5, 6, 7]. In this paper, the voltage-oriented control with cascaded current control and DC voltage control has been chosen. This control scheme is comparable to the field-oriented control of the machine converter:

- Synchronization to: mains voltage position – field position
- Current controller for the space phasor
- DC voltage controller – speed controller

Both VOC and FOC utilize space phasor representation of voltages and currents; space phasor transformation is defined by

$$\underline{v} = \frac{2}{3}\left(v_1 + \underline{a}v_2 + \underline{a}^2 v_3\right) \quad (1)$$

$$\underline{a} = e^{j\frac{2\pi}{3}} \quad (2)$$

$$v_0 = \frac{1}{3}\left(v_1 + v_2 + v_3\right) \quad (3)$$

with respect to a static reference frame. This transformation is power invariant:

Mains voltage line-to-line	400	V rms
Mains frequency	50	Hz
Short-circuit apparent power	35	MVA
Short-circuit power factor	0.2	-
Inductance of mains reactor	400	μH
Resistance of mains reactor	25	mΩ
Nominal AC current	140	A rms
Switching frequency	5	kHz
DC capacitance	30	mF
Nominal DC voltage	693	V

Table 1: System parameters

$$p = \frac{3}{2}\left(+v_{Re}i_{Re} + v_{Im}i_{Im}\right) \quad (4)$$

$$q = \frac{3}{2}\left(-v_{Re}i_{Im} + v_{Im}i_{Re}\right) \quad (5)$$

Transformation of the space phasor to a rotating reference frame (index $_K$) is done according to

$$\underline{v}_K = \underline{v}e^{-j\varphi} \quad (6)$$

$$\varphi = \varphi_0 + \int \omega_K dt \quad (7)$$

However, the product rule of differentiation has to be obeyed, which leads to:

$$\frac{d\underline{i}}{dt} = \frac{d\underline{i}_K}{dt}e^{+j\varphi} + j\omega_K\underline{i}_K e^{+j\varphi} \quad (8)$$

The parameters used for all simulations are summarized in Tab. 1. To achieve more realistic simulations, the grid is not only modeled as a stiff voltage source, but an inductance and a resistance according to the grid's short-circuit apparent power have been added.

2 AFE Modeling

An AFE controls a power conversion bridge such way, that desired AC active and reactive currents are ontained. The following components have been implemneted in a library, additionally summarized in ready-to-use models (Fig. 2):

- AC measurement box `mBoxAC` (subsection 2.1)
- mains reactor `mainsReactor`
- six pulse bridge `b6`, being either an instance of `PowerBalance` or `IdealSwitching` (subsection 2.2)

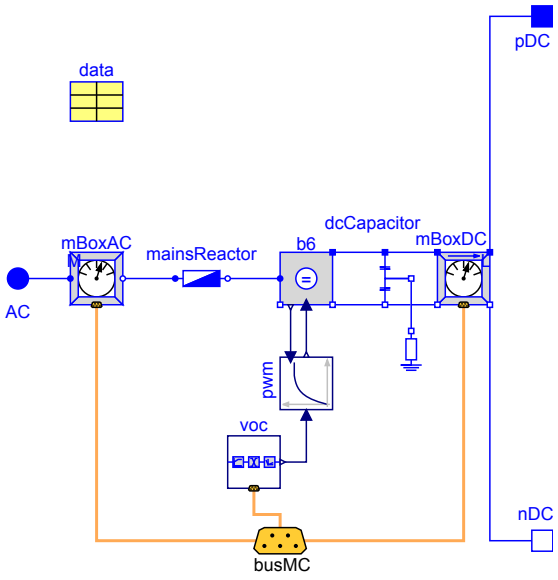

Figure 2: Mains converter with power balance model

- either a `pwmDelay` or a `spaceVectorPWM` block (subsection 2.2)
- buffer capacitor `dcCapacitor`; grounding has to be used carefully, to avoid undefined potentials or short-circuits; therefore, a grounding via a high earthing resistor is included
- DC measurement box `mBoxDC` (subsection 2.3)
- `voc` voltage oriented control block (subsection 2.4)
- `busMC` signal bus (subsection 2.5)
- parameter record `data` (subsection 2.6)

To the signal bus, either a reference input for active and reactive current is required, or a `vDCController` block (subsection 2.7) has to be connected. The DC controller takes the reference parameters or inputs for the set points of the DC voltage and the reactive AC current, controlling the AC active current to obtain the desired DC voltage.

2.1 MBoxAC

The `MBoxAC` measures AC voltages and currents. The voltage can either be measured at the mains terminals (i.e. mains reactor input), or at the converter AC input terminals (i.e. mains reactor output). For the latter case, the voltage drop across the mains reactor is added to the measured converter input voltage to acquire the desired mains voltage.

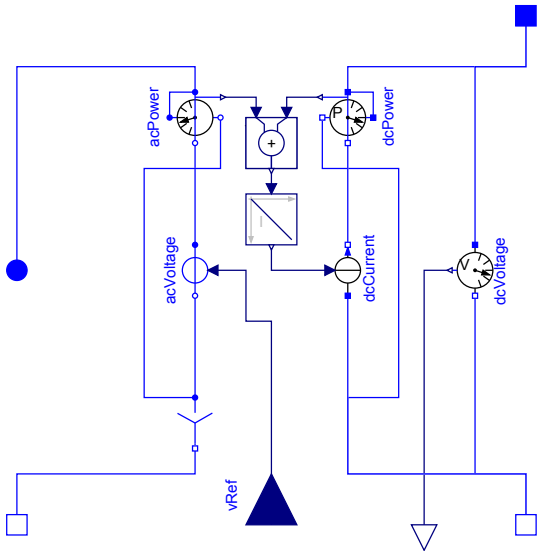

Figure 3: Power Balance model

According to subsection 3.1, reference angle and angular velocity of the mains voltage are determined by means of a synchronization block. Voltages and currents are transformed to space phasors and—using the reference angle—rotated to the voltage oriented reference frame. All quantities are fed to the bus (subsection 2.5).

2.2 Power Conversion Models

2.2.1 Power Balance Model

The `PowerBalance` model (see Fig. 3) consists of a three-phase voltage source, prescribing the AC reference voltages of the current controller. The DC current is determined by an integral power controller, comparing AC power and DC power.

The three-phase reference voltages are pre-processed by a block, limiting the amplitude according to the current DC voltage. Additionally, the reference voltages are delayed by half of a switching period $0.5/f_{PWM}$ to consider the dead time delay of a real PWM. The delay is modeled by means of a PT1 for simplicity reasons.

2.2.2 Ideal Switching Model

The `IdealSwitching` model is built from two three-phase IGBT models (`IdealGTOThyristor`) and two anti-parallel three-phase diodes, taken from the Modelica Standard Library.

The switching states of the IGBTs are determined by a space vector PWM block, as described e.g. in [8] and [9]. Additionally the duty cycles are limited according to the current DC voltage at the beginning of each switching period $1/f_{PWM}$.

phi	reference angle of mains voltage
omega	angular velocity of mains voltage
iRef[2]	space phasor of reference current
iAC[2]	space phasor of actual mains current
vAC[2]	space phasor of actual mains voltage
vDC	actual DC voltage
iDC	actual DC current

Table 2: Bus signals

2.3 MBoxDC

The `MBoxDC` measures DC voltage and current. The current can either be measured between DC capacitor and load terminals, or between converter DC output and DC capacitor terminals. For the latter case, the current drawn by the DC capacitor is added to the measured converter output current to get the desired load current. All measured quantities are fed to the bus (subsection 2.5).

2.4 Current Controller Block

According to subsection 3.2, all components of the current controller have been summarized in this block. The relevant input signals are taken from the control bus (subssection 2.5). The controller output—the three-phase reference voltage—is propagated via a signal output connector.

2.5 Bus

The expandable connector `busMC` contains all signals to be exchanged between measurement models and the different control blocks (Tab. 2). Bus adapters are implemented to connect signal sources for reference values to the bus.

2.6 Parameter Record

This record summarizes all parameters of the ready-to-use models in a convenient way. Additionally, the controller settings (see subsection 3.2 and 3.3) are calculated but can be overwritten by the user, if desired.

2.7 DC Voltage Controller Block

According to subsection 3.3, all components of the DC voltage controller have been summarized in this block.

The desired set point for the DC voltage is defined either as a parameter, or as a signal input. Additionally, the desired reactive reference current can be defined either as a parameter or as a signal input. The controller output—space phasor components of the reference current—are fed to the control bus (subsection 2.5).

3 Controller Design

3.1 Synchronization

Providing a proper synchronization to the base harmonic of the mains voltage even under unbalanced and / or distorted voltage conditions is a crucial task ([10, 11, 12]). Standard solutions use a filter, transform the mains voltages to a space phasor with respect to a static reference frame and rotate this space phasor to the voltage oriented reference frame, using the reference angle that is the output of such a synchronization block. If this rotation is done correctly, the imaginary part of the rotated space phasor should be zero. Thus it could be used as an indicator for a phase locked loop loop (PLL), both determining the angular velocity and the phase angle of the mains voltage space phasor.
Instead of a PLL, the function `Modelica.Math.atan2` is applied to the voltage space phasor with respect to the static reference frame, thus generating the desired phase angle for synchronization. Detecting the mains frequency or rather angular velocity (i.e. the timely derivative of the phase angle) of the space phasor—especially under unbalanced / and or distorted voltage conditions, even with a filter—is much more complicated. In order to keep the models simple, the constant mains frequency is just fed to the bus (subsection 2.5). Since even the ideal switching power conversion model (subsection 2.2.2) causes voltage harmonics when the grid's stiffness is not infinite, a multi variable filter design ([13, 14]) working on the voltage space phasor with respect to the static reference frame is used (Fig. 4).
Analyzing the filter circuit, we can write

$$\frac{d\underline{y}}{dt} = k\left(\underline{u} - \underline{y}\right) + j\omega_N \underline{y}. \tag{9}$$

For a single harmonic with angular frequency ω the frequency response is

$$\frac{\underline{y}}{\underline{u}} = \frac{k}{k + j\left(\omega - \omega_N\right)}. \tag{10}$$

The parameter $k = 2\pi f_B$ defines the bandwidth of the filter. It is obvious that the filter's center frequency

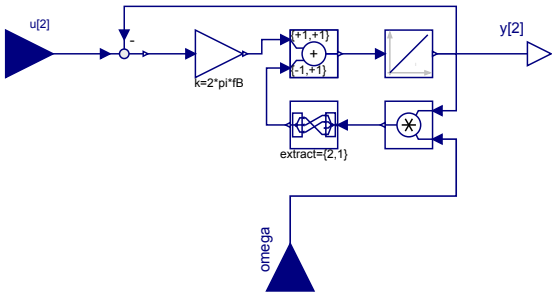

Figure 4: Multi variable filter

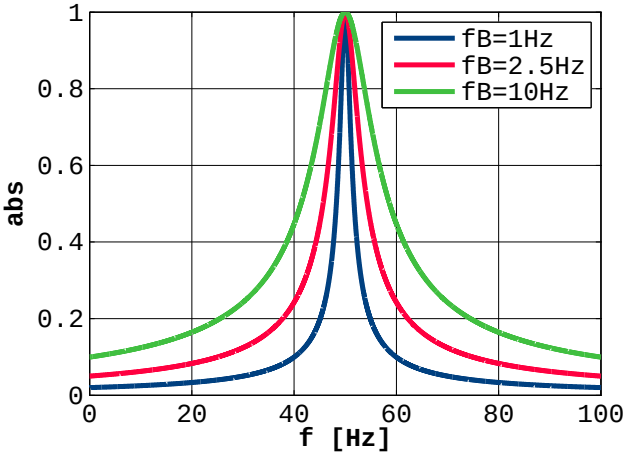

Figure 5: Multi variable filter: gain versus frequency for different bandwidths

ω_N can be adopted simultaneously, e.g. by feeding the current frequency of the PLL. The filter characteristics for various bandwidths are shown in Fig. 5 and 6; at the center frequency gain is 1 and phase shift is 0.

3.2 Current Control Loop

Using the voltage-oriented reference frame, the system can be described using space phasors:

$$\underline{v}_C = \underline{v}_M - R\underline{i} - j\omega L\underline{i} - L\frac{d\underline{i}}{dt} \tag{11}$$

In this equation the index M and C designate the mains and converter side, respectively, and the parameters R and L are the mains resistance and inductance, respecively. Separating the real and imaginary part of this equation and using Laplace transform leads to

$$v_{CRe} = v_{MRe} + \omega L i_{Im} - R\left(1 + s\tau\right) i_{Re}, \tag{12}$$
$$v_{CIm} = v_{MIm} - \omega L i_{Re} - R\left(1 + s\tau\right) i_{Im}, \tag{13}$$

where $\tau = \frac{L}{R}$ is the characteristic time constant.
The complex equation formed by (12) and (13) can be decoupled by means of $\omega L\left(i_{Im} - j i_{Re}\right)$ such

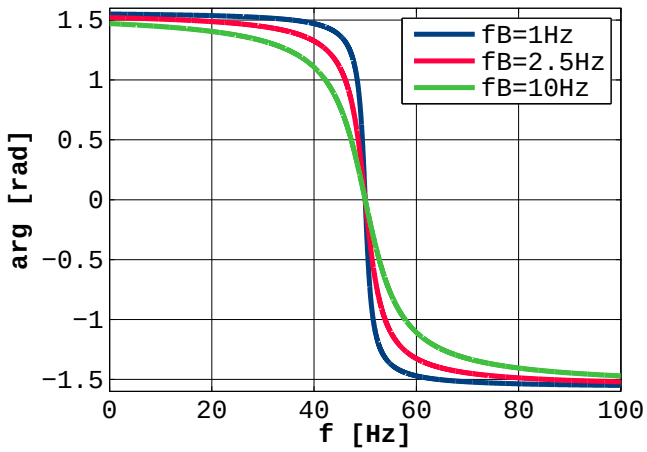

Figure 6: Multi variable filter: phase versus frequency for different bandwidths

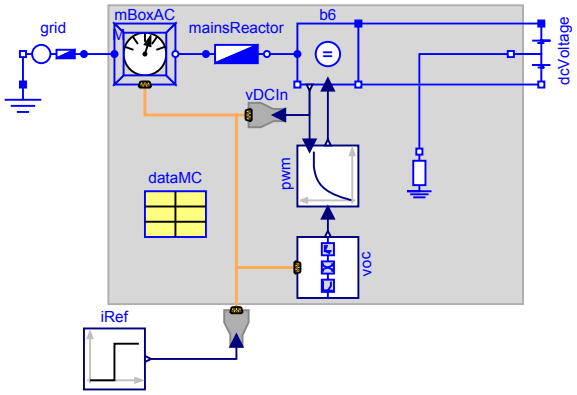

Figure 7: Test example: current control

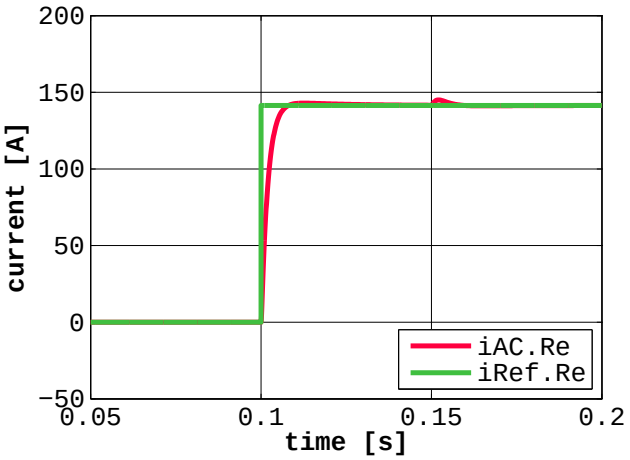

Figure 8: Test example - current control - power balance: real parts of reference current and AC current space phasor

that simple PI controllers can be used for controlling the current. Either measured mains voltage $(v_{MRe} + jv_{MIm})$ can be feed-forwarded, or the integrator states of the PI controllers will meet those values. Compensation of the current's PT1 behavior leads to the controller parameters

$$k_{Current} = k_{DynCurrent}\frac{1}{R}, \quad (14)$$

$$T_{iCurrent} = \tau, \quad (15)$$

where the factor $k_{DynCurrent}$ is used to tune the current controller performance. Neglecting the small dead time delay due to the PWM, the closed current control loop behaves like a PT1 according to

$$i = i_{Ref}\frac{1}{1 + s\tau/k_{DynCurrent}}. \quad (16)$$

The current controller has been investigated with the test example presented in Fig. 7, using the parameters shown in Tab. 1 and a choice of $k_{DynCurrent} = 8$. The gray box emphasizes nearly all components that are included in a ready-to-use model. The DC side of the converter is connected to a constant DC voltage. At time $t = 0.10\,s$, a step of the active reference current of $100\,Arms$ (i.e. a real part of the reference space phasor of $\sqrt{2} \cdot 100\,A$), and at time $t = 0.15\,s$, a step of the reactive reference current of $-100\,Arms$ (i.e. imaginary part of the reference space phasor of $\sqrt{2} \cdot 100\,A$) is applied.

Fig. 8 and 9 show the real and the imaginary part of the reference and AC current space phasor. Replacing the power balance model `b6` by an ideal switching model, as well as the delay component `pwm` by a space vector PWM block, the results in Fig. 10 and 11 are obtained. The comparison of the power balance and the switching models, however, shows the same qualitative behavior.

3.3 DC Voltage Controller

To describe the relationship between DC voltage, load current and mains current, power balance

$$p_{AC} = \frac{3}{2}v_{MRe}i_{Re} = p_{DC} = v_{DC}i_{DC} \quad (17)$$

can be used, neglecting the losses of the mains inductor (17). Compared with (4), we see that due to the usage of the voltage oriented reference frame, $v_{MIm} = 0$. Thus we can derive the factor between the real part of the AC current space phasor and the DC

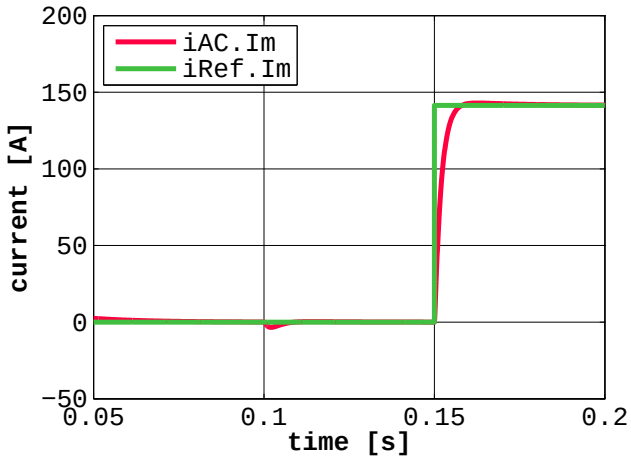

Figure 9: Test example - current control - power balance: imaginary parts of reference current and AC current space phasor

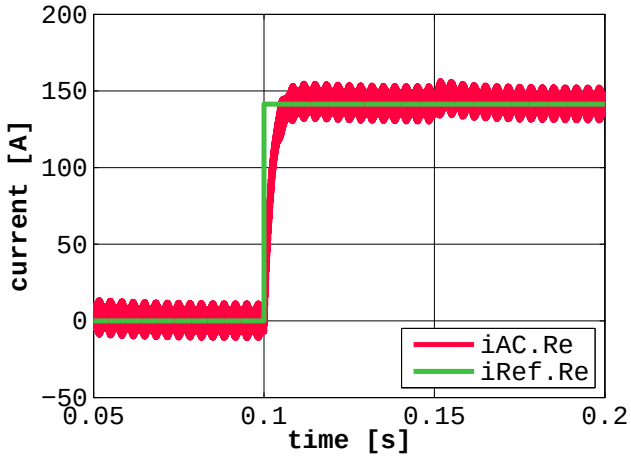

Figure 10: Test example - current control - ideal switching: real parts of reference current and AC current space phasor

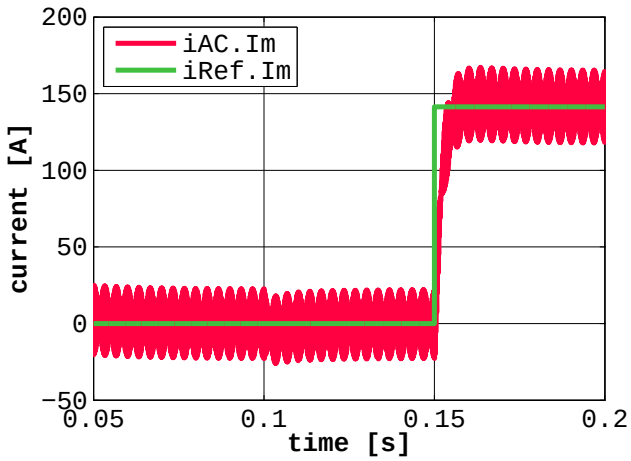

Figure 11: Test example - current control - ideal switching: imaginary parts of reference current and AC current space phasor

load current for stationary operation:

$$k_{ACDC} = \frac{i_{DC}}{i_{AC,Re}} = \sqrt{\frac{3}{2}} \frac{V_{AC,rms,line-to-line,Nominal}}{V_{DC,Nominal}} \tag{18}$$

Using Laplace transform and taking the reference tracking performance of the current control loop (16) into account, we obtain:

$$k_{ACDC} \frac{i_{Ref,Re}}{1 + s\tau/k_{DynCurrent}} = i_{DC,load} + sC_{DC}v_{DC} \tag{19}$$

Using factor $k_{DynVoltage}$ to tune the performance of the DC voltage controller, we choose a PI controller, parametrized according to the symmetrical optimum (standard choice $a = 2$). The gain and time constant of this controller are:

$$k_{Voltage} = k_{DynVoltage} \frac{C_{DC}}{k_{ACDC}} \frac{a}{T_{iVoltage}} \tag{20}$$

$$T_{iVoltage} = a^2\tau/k_{DynCurrent} \tag{21}$$

The measured load current can bee feed-forwarded to enhance the performance of the DC voltage controller. The DC voltage controller has been investigated with the test example presented in Fig. 12, using the parameters shown in Tab. 1, choices of $k_{DynCurrent} = 8$ and $k_{DynDCVoltage} = 2$, and with feed-forward of the measured DC load current. The gray box emphasizes all components that are included in a ready-to-use model. The reference of the DC voltage has been set to nominal DC voltage, the reference of the reactive AC current has been set to zero. At time $t = 0.10\,\mathrm{s}$, the DC side is loaded with a constant power of $v_{DC,Nominal} \cdot 100\,A$.

Fig. 13 shows the DC voltage and Fig. 14 show the real part of the reference and the AC current space phasor. Replacing the power balance model `b6` by an ideal switching model, as well as the delay component `pwm` by a space vector PWM block, the results Fig. 15 and 16 are obtained. The comparison of the power balance and the switching models, however, shows the same qualitative behavior.

4 Complete Example

Finally, the ready-to-use models have been investigated with the test example depicted in Fig. 17, using the parameters shown in Tab. 1, $k_{DynCurrent} = 8$, $k_{DynDCVoltage} = 2$, and without feed-forward of the measured DC load current. A DC voltage controller

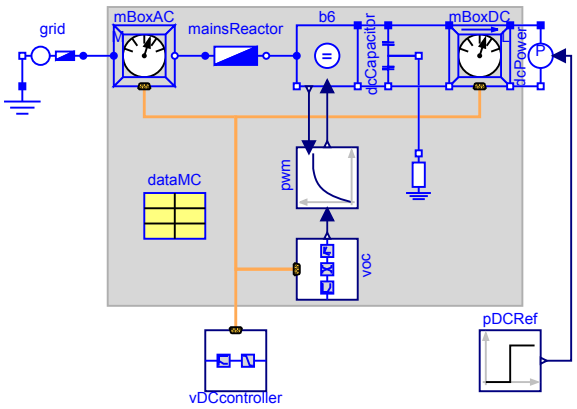

Figure 12: Test example: DC voltage control

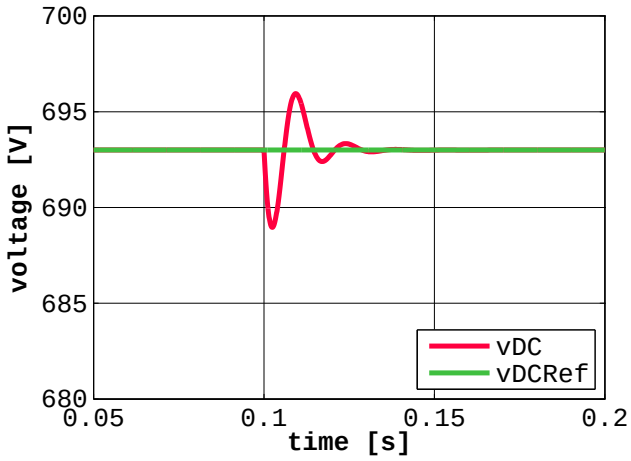

Figure 13: Test example - DC voltage control - power balance: reference and actual DC voltage

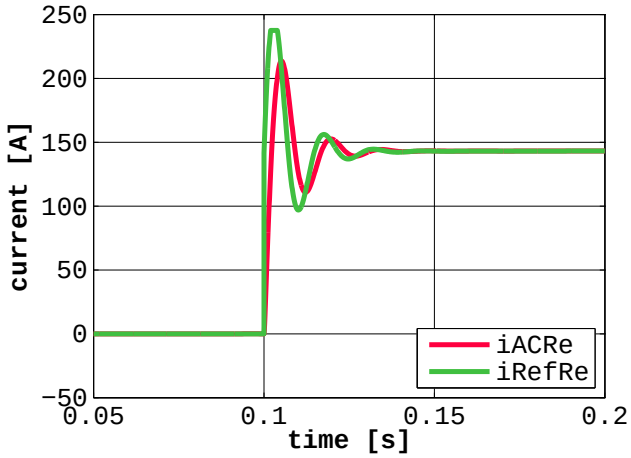

Figure 14: Test example - DC voltage control - power balance: real parts of reference current and AC current space phasor

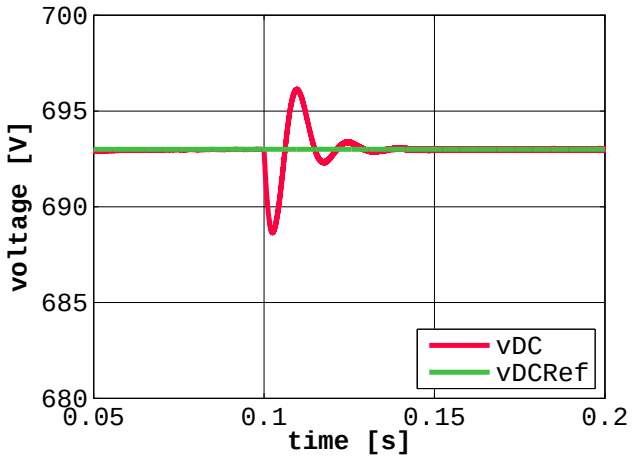

Figure 15: Test example - DC voltage control - ideal switching: reference and actual DC voltage

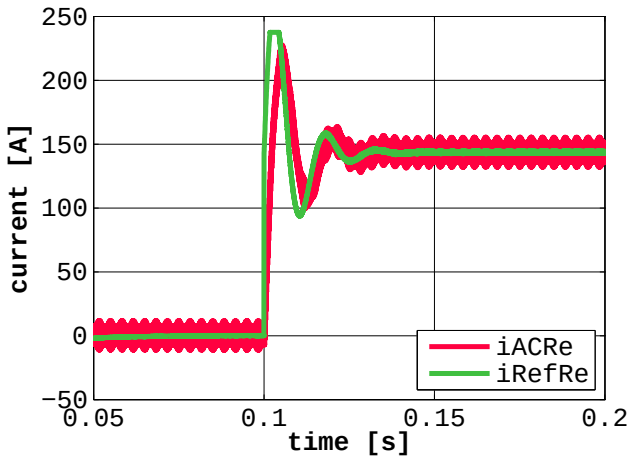

Figure 16: Test example - DC voltage control - ideal switching: real parts of reference current and AC current space phasor

is connected to mains converter `mc1`; mains converter `mc2` controls active and reactive current, thus creating a DC load for mains converter `mc1`. At time $t = 0.10\,s$, a step of the active reference current of $100\,A$ (i.e. a real part of the reference space phasor of $\sqrt{2} \cdot 100\,A$) is applied to the mains converter `mc2`; the set point of reactive reference current remains 0. The AC terminals of both mains converters are connected to the same mains, thus the grid delivers only active current to cover losses (of the mains reactors). Since both converter models contain a DC capacitor (which is initialized at nominal DC voltage), the DC terminals have to be connected via small bus bar resistances.

Fig.18 shows real parts of reference and AC current space phasor of mains converter `mc2`. The resulting real parts of reference and AC current space phasor of

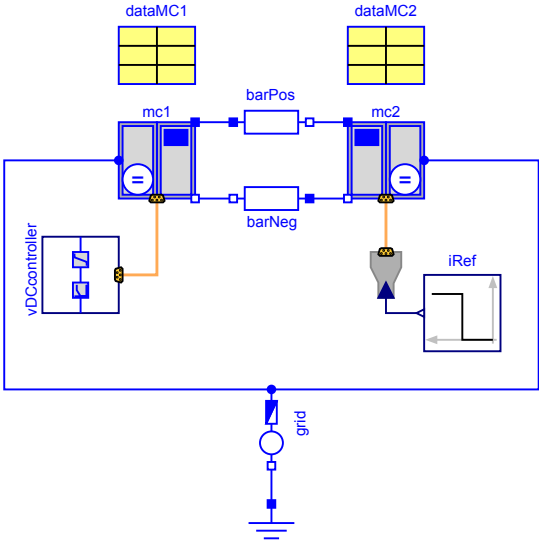

Figure 17: Complete example

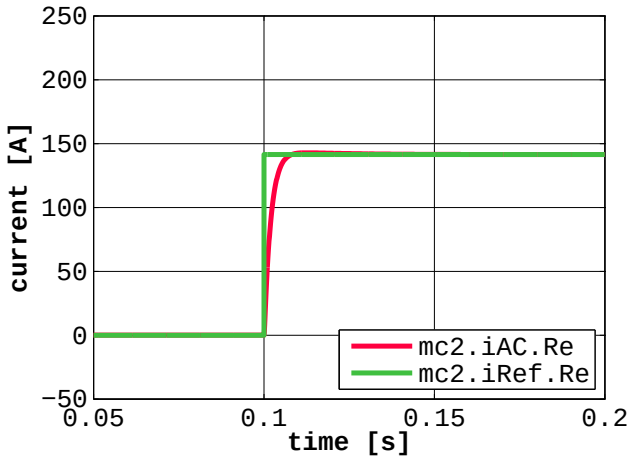

Figure 18: Complete example - power balance, Converter2: real parts of reference current and AC current space phasor

mains converter `mc1` are depicted in Fig. 19. DC voltage is controlled very well, as demonstrated in Fig. 20. Replacing the power balance models `mc1` and `mc2` by ideal switching models, the results Fig. 21–23 have been obtained. The comparison of the power balance and the switching models, however, shows the same qualitative behavior.

5 Conclusions

All components needed to implement ready-to-use models of an AFE, i.e. a mains connected PWM converter with voltage oriented control, have been presented and tested by means of simulations. A complete example demonstrates the usage of the ready-to-use

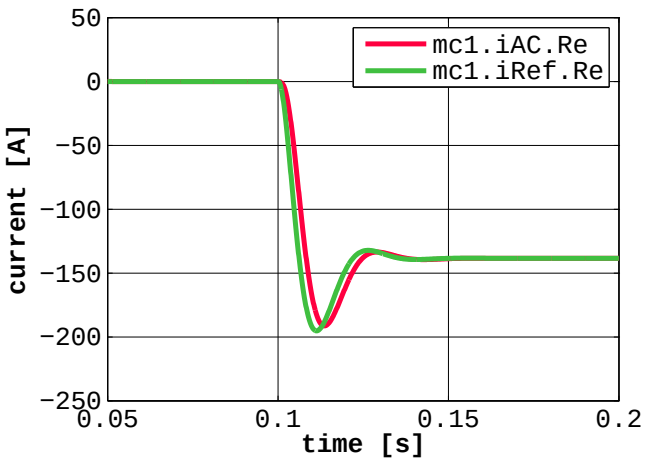

Figure 19: Complete example - power balance, Converter1: real parts of reference current and AC current space phasor

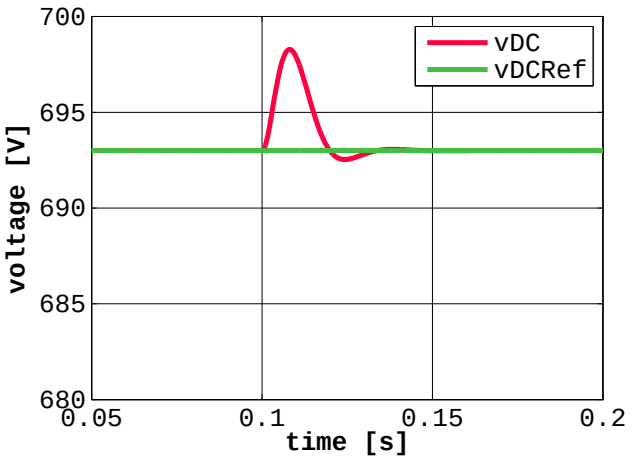

Figure 20: Complete example - power balance: reference and actual DC voltage

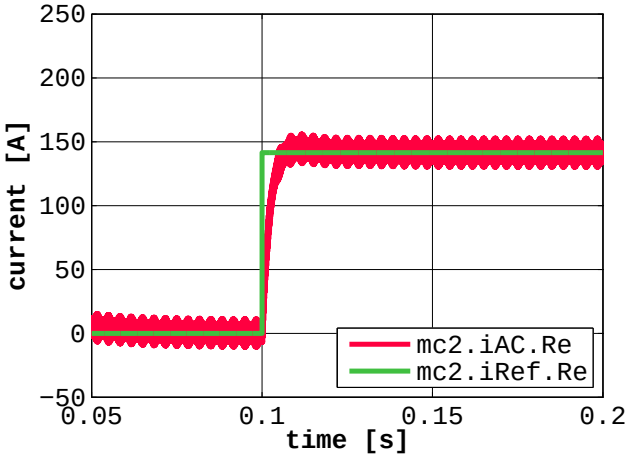

Figure 21: Complete example - ideal switching, Converter2: real parts of reference current and AC current space phasor

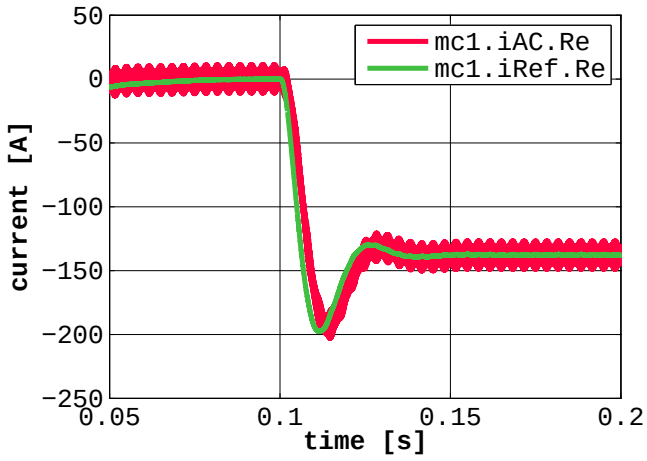

Figure 22: Complete example - ideal switching, Converter1: real parts of reference current and AC current space phasor

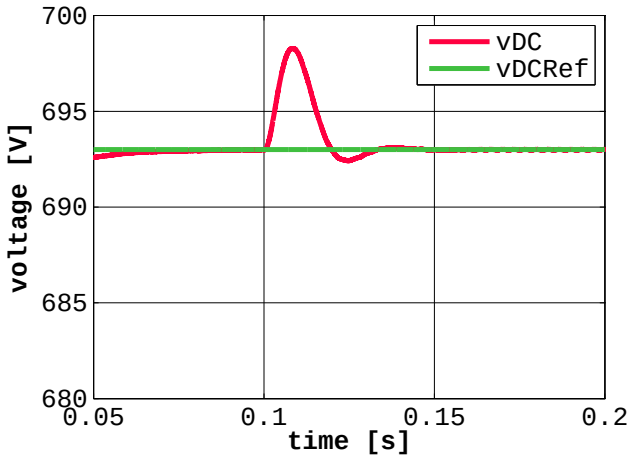

Figure 23: Complete example - ideal switching: reference and actual DC voltage

models. The user can choose between a power balance model and an ideal switching model. As expected, the power balance model—neglecting switching effects—speeds up simulation by a factor of more than 100, of course dependent on the PWM switching frequency. Using these AFE models, a lot of investigations can be carried out, like:

- Behavior of the AFE under unbalanced or distorted mains voltage
- Parallel operation of AFEs at the same DC bus
- Stability of an AFE under weak grid conditions or connected to a synchronous generator
- Implementation of power controllers for wind turbines or solar converters
- Usage of an AFE as reactive power compensation

Further development is planned for:

- Coupling the AFE models with drive models from the `SmartElectricDrives` library
- Enhancing the synchronization
- Adapting current control to mains-side LCL filters

References

[1] J. V. Gragger, H. Giuliani, C. Kral, T. Bäuml, H. Kapeller, and F. Pirker, "The SmartElectricDrives Library – powerful models for fast simulations of electric drives," *The 5th International Modelica Conference*, pp. 571–577, 2006.

[2] M. Malinowski, M. Kazmierkowski, and A. Trzynadlowski, "Review and comparative study of control techniques for three-phase pwm rectifiers," *Mathematics and Computers in Simulation*, vol. 63, p. 349–361, 2003.

[3] M. Malinowski, M. P. Kazmierkowski, and A. M. Trzynadlowski, "A comparative study of control techniques for pwm rectifiers in ac adjustable speed drives," *IEEE Transactions On Power Electronics*, vol. 18, no. 5, pp. 1390–1396, May 2003.

[4] S. L. Sanjuan, "Voltage oriented control of three-phase boost pwm converters," Master's thesis, Chalmers University of Technology, Gothenburg, 2010.

[5] F. Blaabjerg, R. Teodorescu, Z. Chen, and M. Liserre, "Power converters and control of renewable energy systems," *International Conference on Power Electronics, ICPE 2004*, pp. 2–20, 2004.

[6] T. Østrem, "Reliable electric power conversion for connecting renewables to the distribution network," Ph.D. dissertation, Norwegian University of Science and Technology, 2008.

[7] S. E. Evju, "Fundamentals of grid connected photovoltaic power electronic converter design," Master's thesis, Norwegian University of Science and Technology, 2007.

[8] J. V. Gragger, A. Haumer, C. Kral, and F. Pirker, "Efficient analysis of harmonic losses in PWM voltage source induction machine drives with Modelica," *International Modelica Conference, 6th, Bielefeld, Germany*, pp. 593–600, 2008.

[9] A. Boglietti, G. Griva, M. Pastorelli, F. Profumo, and T. Adam, "Different PWM modulation techniques indexes performance evaluation," *IEEE International Symposium on Industrial Electronics, ISIE'93 - Budapest.*, pp. 193–199, 1993.

[10] F. D. Freijedo, J. Doval-Gandoy, O. Lopez, C. Martinez-Penalver, A. G. Yepes, P. Fernandez-Comesana, J. Malvar, A. Nogueiras, J. Marcos, and A. Lago, "Grid-synchronization methods for power converters," *35th Annual Conference of IEEE Industrial Electronics, IECON 2009*, pp. 522–529, 2009.

[11] A. Nagliero, R. A. Mastromauro, M. Liserre, and A. Dell'Aquila, "Synchronization techniques for grid connected wind turbines," *35th Annual Conference of IEEE Industrial Electronics, IECON 2009.*, pp. 4606–4613, 2009.

[12] A. Timbus, R. Teodorescu, F. Blaabjerg, and M. Liserre, "Synchronization methods for three phase distributed power generation systems. an overview and evaluation," *IEEE 36th Power Electronics Specialists Conference, PESC 2005.*, pp. 2474 – 2481, 2005.

[13] T. Østrem, W. Sulkowski, L. E. Norum, and C. Wang, "Grid connected photovoltaic (pv) inverter with robust phase-locked loop (pll)," *IEEE PES Transmission and Distribution Conference and Exposition Latin America*, 2006.

[14] M. C. Benhabib, F. Wang, and J. L. Duarte, "Improved robust phase locked loop for utility grid applications," *13th European Conference on Power Electronics and Applications, EPE 2009*, pp. 1–8, 2009.